Optica Applicata, Vol. XXXVII, No. 3, 2007

The behavior of the Poynting vector in the area of elementary polarization singularities

I. MOKHUN, R. KHROBATIN, A. MOKHUN, JU. VIKTOROVSKAYA

Chernivtsi National University, 12, Kotsybinski str, Chernivtsi 58012, Ukraine

The behavior of the Poynting vector in the area of elementary polarization singularities with one or two *C*-points, which are bounded by regular shape *s*-contour is considered. It has been shown that *C*-points are associated with the "vortex" kind singularities of the averaged transversal component of the Poynting vector if the handedness factor and topological charge of *C*-point are characterized by different signs. "Passive" Poynting singularities arise in the area if the signs are the same. It has been shown that the positions of the Poynting singularities shift relatively to the *C*-points under the phase and amplitude asymmetry of orthogonal components of the resulting field. The results of the computer simulation are presented.

Keywords: angular momentum, Poynting vector, polarization, vortex, polarization singularities, *s*-contour, *C*-point.

1. Introduction

One of the theoretical aspects of the rapidly developing area of modern optical technology – elaboration of new kinds of optical tweezers [1] – is connected with the fact that vortex beams, polarized waves (both homogeneous and heterogeneous ones) possess an angular momentum [1–3]. The appearance of a controlled angular momentum provides the possibility of the controlled rotation of the micro objects locked by corresponding optical traps. An angular momentum of a field may be considered in each space point. An averaged angular momentum may be also considered for some space area. As it is well known the angular momentum may be decomposed into the spin angular momentum associated with elliptical polarization and the orbital one that is produced by the structure of a beam (see, for example, [2, 4]). However, such angular momentum is characterized by not only the magnitude, but also by the point of "applying". As a result some ambiguity appears. At the same time, another physical quantity closely connected with the angular momentum, namely the space distribution of the Poynting vector characteristics (or rather its transversal component) is a univocal function of the coordinates of each field point.

Distribution of the Poyinting vector parameters for Laguerre–Gaussian beams was considered in [5, 6]. However, only the behavior of an averaged Poynting vector for

a homogeneously polarized field and "symmetrical" beams was analyzed [2, 5]. Therefore, in our opinion the problem must be investigated in more details. The reasons of this are the following:

1. The angular momentum of the heterogeneously polarized field of more general kind must be investigated.

2. The behavior of an instantaneous Poynting vector must be considered because the analysis of the averaged one has some sense only in the case when the field influences the physical system with relaxation time which is significantly longer than the vibration period of a wave. Such condition is practically always satisfied for optical waves, whereas for a radio wave band it becomes problematic.

3. In our opinion, at least, for the heterogeneously polarized fields, the decomposition of the total angular momentum into the spin angular momentum, and the orbital one has no physical sense.

4. As the space distributed volumes, Poynting vector parameters have singular and stationary points. Information about the system of such points, their topological characteristics, and relationships between them, give us the possibility to predict the qualitative behavior of the Poynting vector at each field point and make the influence of the electromagnetic wave on the physical system clear to us.

The characteristics of the distributions of the Poynting vector of relatively simple heterogeneously polarized fields are considered in this paper. Instantaneous and averaged Poynting vectors, their singularities "determining" the point of "applying" of the averaged angular momentum, regularities of their singularities system formation and their relationship with conventional polarization singularities (*C*-points and *s*-contours) [7] are analyzed.

2. General assumptions

Let us assume that the paraxial approximation is satisfied. Only the fields which contain the minimal number (one or two) of *C*-points (points where a field is circularly polarized [7]) will be considered. Heterogeneously polarized area is limited by *s*-contour (line along which a field is linearly polarized [7]) of a relatively regular shape. Such field may be formed by the superposition of the vortex circular polarized beam and of the orthogonally polarized smooth one [3, 8, 9]. *C*-points are located in the vortex centers positions and *s*-contour is formed along the line where beams have equal intensities. *C*-point topological charge of the vibration phase S_C, its Poincare index I_C (or simply *C*-point index) are defined by the topological charge of the "forming" vortex [10]:

$$\begin{cases} S_C = \dfrac{1}{2} S \\ I_C = h S_C \end{cases} \tag{1}$$

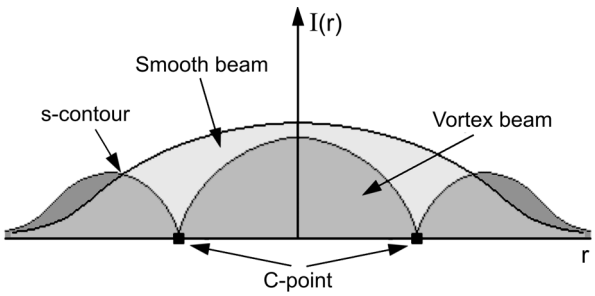

Fig. 1. Formation of the simple heterogeneously polarized field.

where h – the handedness factor which is equal to ±1 for right-hand and left-hand polarization regions, respectively; S – the topological charge of the vortex in the vortex circularly polarized beam.

One of the possible behaviors of the superposing beams intensities is illustrated in Fig. 1. As it follows from the figure, the *C*-point is positioned at the point where the vortex component has exact zero of its amplitude [7].

It has been shown [3] that the instantaneous components of the Poynting vector may be written as the following relations:

$$\begin{cases} P_x \approx -\dfrac{c}{4\pi k}\left(E_x T_2 - E_y T_1\right) \\ P_y \approx -\dfrac{c}{4\pi k}\left(E_y T_2 + E_x T_1\right) \\ P_z \approx \dfrac{c}{4\pi}\left(E_x^2 + E_y^2\right) \end{cases} \tag{2}$$

where

$$\begin{cases} T_1 = E_x \Phi_x^y - E_y \Phi_y^x + \dfrac{e_x^y}{e_x} E_{x,\frac{\pi}{2}} - \dfrac{e_y^x}{e_y} E_{y,\frac{\pi}{2}} \\ T_2 = E_x \Phi_x^x + E_y \Phi_y^y + \dfrac{e_x^x}{e_x} E_{x,\frac{\pi}{2}} + \dfrac{e_y^y}{e_y} E_{y,\frac{\pi}{2}} \end{cases} \tag{3}$$

and

$$\begin{cases} E_i = e_i \cos(\omega t + \Phi_i - kz) \\ E_{i,\frac{\pi}{2}} = e_i \sin(\omega t + \Phi_i - kz) \end{cases} \tag{4}$$

e_i, Φ_i – the amplitudes and component phases, respectively; e_i^l, Φ_i^l – their derivatives and i, $l = x, y$; $k = 2\pi/\lambda$ – the wave number; ω – the circular frequency of light vibration; c – light speed.

The computer simulation was performed on the basis of these relations and on the basis of the averaged in time version of them.

3. Polarization cell with one *C*-point. Angular momentum in the area of *C*-point

The polarization cell with one *C*-point may be obtained in the following way. Let us assume that the vortex beam is the circular polarized isotropic vortex [11] and the smooth beam is the orthogonally polarized plane wave.

The complex amplitudes of the vortex beam and the smooth beam (in terms of linearly polarized orthogonal components) may be represented in the following form, respectively:

$$\begin{cases} U_{Vx} = \rho \exp(jS\varphi) \\ U_{Vy} = \rho \exp\left[j\left(S\varphi + h\dfrac{\pi}{2}\right)\right] \end{cases} \tag{5}$$

$$\begin{cases} U_{Rx} = 1 \\ U_{Ry} = \exp\left(-jh\dfrac{\pi}{2}\right) \end{cases} \tag{6}$$

where φ and $\rho = \sqrt{x^2 + y^2}$ are the polar coordinates whose origin coincides with the vortex center; S – the topological charge of the vortex.

It can be shown that after little algebra on the basis of Eqs. (2)–(4) the instantaneous transversal components of the Poynting vector may be written as [3]:

$$\begin{cases} P_x = -\dfrac{c}{4\pi k}\left\{\dfrac{1 - Sh}{S - h}\sin\left[2(\omega t - kz)\right] - y\right\}(S - h) \\ P_y = -\dfrac{c}{4\pi k}\left\{\cos\left[2(\omega t - kz)\right] + x\right\}(S - h) \end{cases} \tag{7}$$

It can be seen that $P_x, P_y = 0$, when $S = h$. In the opposite case ($S = -h$) we obtain:

$$\begin{cases} P_x = -\dfrac{c}{4\pi k} 2S \left\{ S \sin\left[2(\omega t - kz)\right] - y \right\} \\ P_y = -\dfrac{c}{4\pi k} 2S \left\{ \cos\left[2(\omega t - kz)\right] + x \right\} \end{cases} \tag{8}$$

Accordingly [2, 4], z-component of angular momentum density is given by the following relation:

$$j_z = xP_y - yP_x \tag{9}$$

It can be shown that the following relation for the averaged angular momentum for the case $S = -h$ may be obtained on the basis of Eqs. (8) and (9):

$$\overline{M} = -\frac{2S_C c^2}{\omega} J \tag{10}$$

where $J = \int_0^{\rho_0} \rho^2 \mathrm{d}\rho$ is defined by the "power" of the vortex beam in the actual area of the cell with diameter $2\rho_0$. Thus, the averaged angular momentum appears in the C-point vicinity when the signs of the vortex topological charge and handedness factor are different. In other words, the following relation must be satisfied for the angular momentum appearance with the point of application in the C-point position:

$$S = 2S_C = -h \tag{11}$$

The Poynting singularity may appear in two cases:

– all three components vanish simultaneously; this case corresponds to the appearance of the Nye's disclination [7, 12, 13];

– only transversal component vanishes; this case corresponds to simultaneous vanishing of T_1 and T_2 (see Eq. (2)). Really, in this case, the orientation of the transversal component of the Poynting vector (its azimuth $\theta = \arctan(P_y/P_x)$) is indeterminate.

Figure 2 presents the behavior of the instantaneous transversal component of the Poynting vector obtained for polarization cell, defined by Eqs. (5) and (6). Distributions were calculated for the set of moments with the step equal to 1/8 of vibration period.

It can be seen, from Figure 2, that the Poynting singularity corresponding to the disclination moves along a circular s-contour. C-point is positioned in the center of the area bounded by it. It has been noted that the maximal angular momentum averaged over small time δt and over small area in the vicinity of this singularity is the angular momentum with the application point just in this singularity. The Poincare

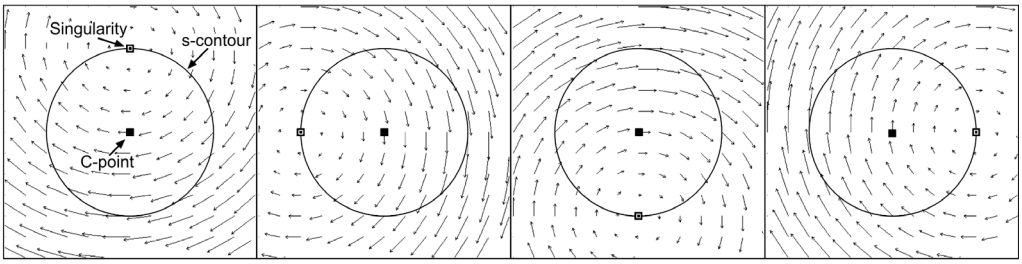

Fig. 2. The behavior of the instantaneous transversal component of the Poynting vector. Orientation of the component is represented by arrows. The modulus of this vector corresponds to the length of arrows. Singularity moves along *s*-contour in a counterclockwise direction.

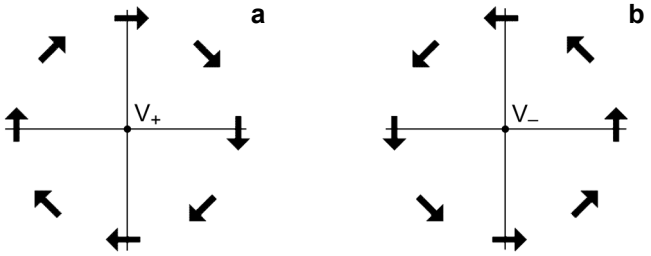

Fig. 3. Circulation of the Poynting vector transversal component around the vortex singularity.

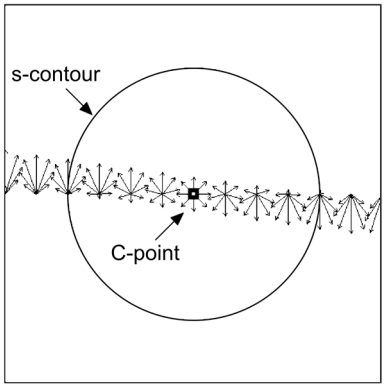

Fig. 4. The behavior of the transversal component for different moments and for points localized along one of the diameters of *s*-contour. The orientation of the component is represented by arrows. The modulus of this vector corresponds to the length of arrows.

index (calculated for the azimuth changes of the vector) characterizes this singularity. Let us call such singularity a "vortex" one due to the similarity of the Poynting vector "circulation" around the center of a common phase vortex [2]. It has been noted that the index equal to +1 corresponds to both possible different directions of vector circulation. Therefore, the additional parameter like chirality must be introduced for complete characterization of such Poynting vector azimuth singularity.

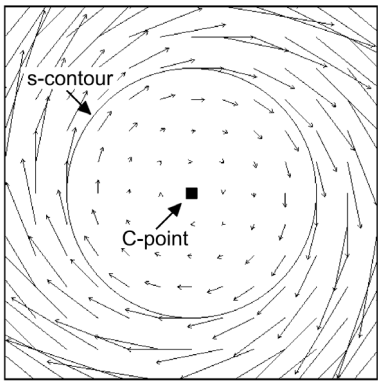

Fig. 5. The behavior of the averaged transversal Poynting vector component in the vicinity of *C*-point. The orientation of the component is represented by arrows. The modulus of this vector corresponds to the length of arrows.

Let us assume that the field propagates toward the observer. Let the positive chirality $V = +1$ (*cf.* Fig. 3**a**) correspond to the clockwise vector circulation, and the negative chirality $V = -1$ (*cf.* Fig. 3**b**) correspond to the counterclockwise vector circulation.

The behavior of the transversal component for different moments and for points localized along one of the diameters of *s*-contour is illustrated in Fig. 4. Obviously, the averaged transversal component of the Poyinting vector will be equal to zero in the *C*-point position and its magnitude will increase toward the *s*-contour.

The behavior of averaged transversal Poynting vector component is illustrated in Fig. 5. It can be seen that the averaged vector behavior presented is very similar to the one associated with the Poynting vector circulation in the vicinity of the common phase vortex. However, in the vortex center all three components of the averaged Poynting vector are equal to zero, whereas *z*-component is non-zero in our case. Thus, the energy current is absent along the zero line (3-D loci of vortex center) and it is maximum, as a rule, along the *z*-axis in our case.

It has been noted that the light optical trap with orbital angular momentum may be formed by focusing of such beam superposition [3].

4. Polarization cell with two *C*-points. *C*-points of the same signs

Polarization cell with two *C*-points of the same signs may be obtained by superposition of a circularly polarized vortex beam with two identical vortices and an orthogonally polarized plane wave.

Figure 6 illustrates the structure of the phase of the vortex beam. The *s*-contour forming under superposition is also denoted in the figure by a white closed curve.

Accordingly [12, 13], two disclinations appear on the *s*-contour (see Fig. 7). It can be shown that the structures of these disclinations are absolutely the same. As a result, the structures of the Poynting singularities must be also the same.

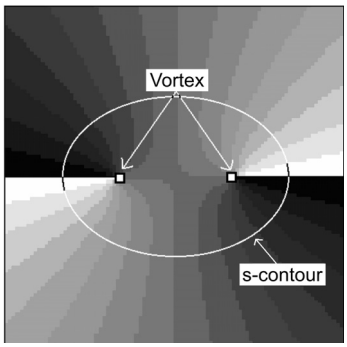

Fig. 6. A phase map of the vortex beam. Different colors corresponds to different (within 2π) phases. The position of the *s*-contour is represented by the white line.

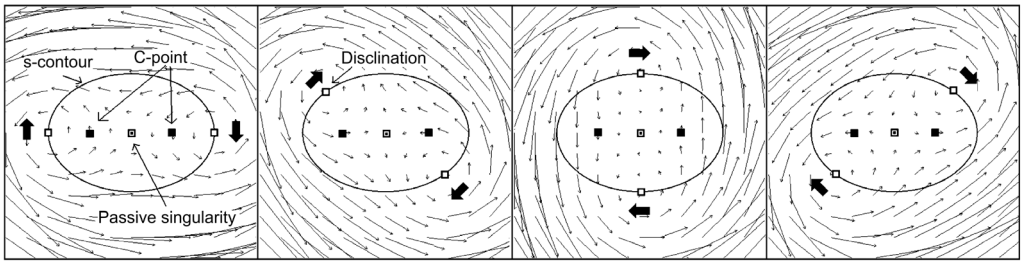

Fig. 7. Distribution of the Poynting vector azimuth for the field, which contains two *C*-points with the same signs. The direction of singularities motion is represented by thick arrows.

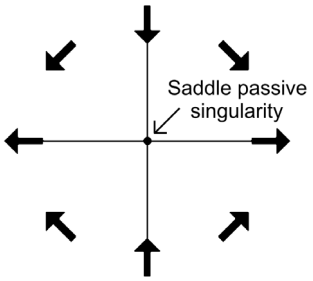

Fig. 8. Passive singularity. The orientation of the Poynting vector transversal component in the vicinity of such singularity.

Two vortex singularities associated with disclinations move along the *s*-contour. It has been noted that an additional Poynting singularity arises in the geometrical center of the area. Such additional singularity topologically connects Poynting vortices together. This is a saddle-like singularity of the Poynting vector azimuth. We will call it a "passive" singularity, because the angular momentum, averaged over small time δt, is equal to zero in its small area.

The behavior of the transversal component of the Poynting vector in the area of such singularity is illustrated in Fig. 8. Negative Poincare index characterizes this vector azimuth singularity.

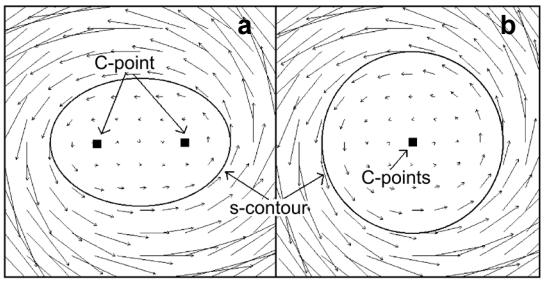

Fig. 9. The behavior of the Poynting vector for the cell with two spatially divided *C*-points – **a**; the space between two *C*-points is small – **b**. The magnitude of the vector modulus is represented by the length of arrows.

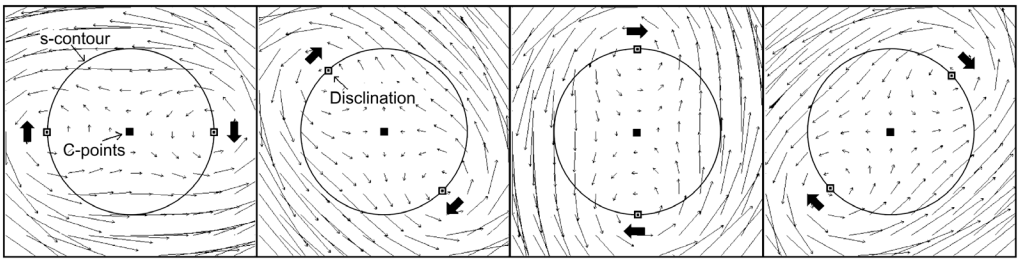

Fig. 10. Distributions of the instantaneous Poynting vector azimuth for the field, which contains two closely positioned *C*-points with the same signs. Direction of the singularities motion is represented by thick arrows.

The behavior of the averaged Poynting vector is illustrated in Fig. 9. It can be seen that such behavior (see Fig. 9**a**) differs slightly from the one corresponding to the cell with one *C*-point. Such azimuth distribution is practically the same if the space between *C*-points is small (see Fig. 9**b**). Nevertheless two instantaneous Poynting vortices are observed for the temporal behavior of the instantaneous Poynting vector. Corresponding distributions calculated for the set of moments with the step equaled to 1/8 of vibration period are presented in Fig. 10. The magnitude of the vector modulus is represented by the length of arrows.

5. Polarization cell with two *C*-points. *C*-points of different signs

Polarization cell with two *C*-points of different signs may be obtained by the superposition of a circularly polarized vortex beam with two vortices with opposite signs and an orthogonally polarized plane wave.

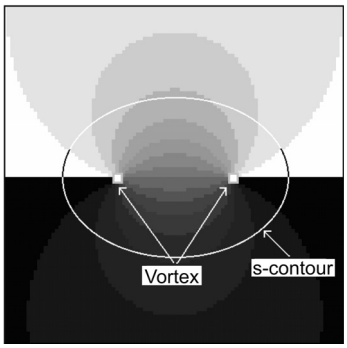

Fig. 11. A phase map of the vortex beam. Different colors correspond to the different (within 2π) phases. The position of the *s*-contour is denoted by the white line.

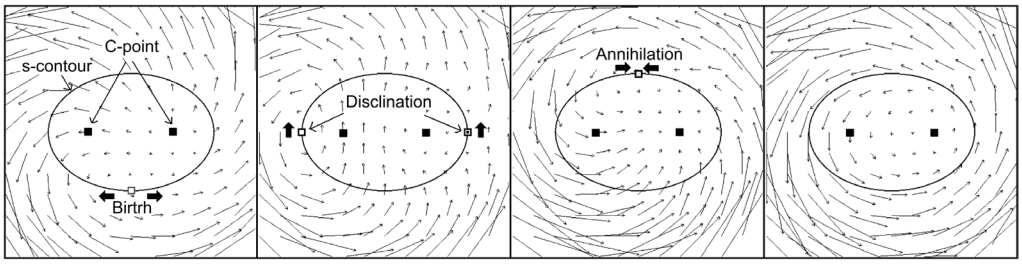

Fig. 12. Distributions of the instantaneous Poynting vector azimuth for the field, which contains two *C*-points with different signs. The magnitude of the vector module is represented by the length of arrows. Direction of the singularities motion is represented by thick arrows.

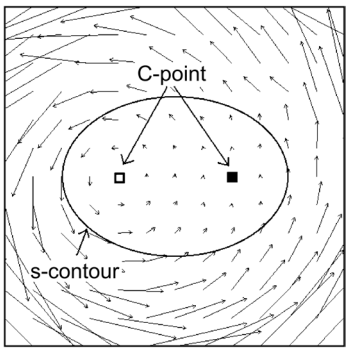

Fig. 13. The behavior of the transversal component of the averaged Poynting vector for the cell with the *C*-points of different signs.

The phase structure of the circularly polarized vortex beam and the position of *s*-contour of the resulting field are illustrated in Fig. 11. It can be seen that *s*-contour remains in the location denoted in Fig. 6.

Two Poynting singularities appeared, like in the case of the *C*-points of the same signs. However, they have different chiralities and these singularities move in opposite directions. From Fig. 12 (temporal step is the same like for Figs. 7 and 10) it can be

seen that the birth and annihilation events are observed at some moments and only when Poynting singularities are absent in the area.

The behavior of the azimuth of the averaged Poynting vector is illustrated in Fig. 13. The magnitude of the vector modulus is represented by the length of arrows. It can be seen that the modulus of the Poynting vector is practically zero in the area of *C*-point which has the sign of the topological charge of the vibration phase equal to the sign of the handedness factor $S_C = h/2$ (right *C*-point), while the vortex singularity is observed in the left *C*-point position.

6. "Non symmetrical" distributions

From the performed analysis it can be assumed that the positions of vortex singularities associated with the transversal component of the averaged Poynting vector coincide with positions of *C*-points. As a result, the points of applying the averaged field angular momentum also coincide with these points. However, this statement is not always true. This fact takes place only in the case, namely when interfering beams have symmetrical (relatively to the center of the resulting beam) distributions of amplitudes and phases.

Let us show that perturbation of amplitude and phase symmetry leads to the shift of the singularity point relatively to the *C*-point position. It can be shown that a principal factor is not associated with the magnitude of asymmetry between single beams, but with the mutual changes of phase difference and amplitude ratio gradients. Similarly, as it is well known, the identical changes of phases of the interfering beams (even significant ones) do not result in bending of interference fringes of the resulting pattern in a conventional interference experiment. Thus, let us assume that asymmetry is introduced only in one beam, namely in the reference one.

It can be shown that in this case (the complex amplitude of the vortex beam is given by Eq. (5)) the averaged components of the Poynting vector are given by the following relations:

$$\begin{cases} \overline{P}_x = -\dfrac{c}{4\pi k} A^2 \left[\dfrac{h-S}{A^2} y + \Phi^x - h \dfrac{A^y}{A} \right] \\ \overline{P}_y = -\dfrac{c}{4\pi k} A^2 \left[\dfrac{h-S}{A^2} x + \Phi^y - h \dfrac{A^x}{A} \right] \end{cases} \tag{12}$$

where Φ^x, Φ^y – the phase derivatives; A – the amplitude of the reference beam; A^x/A and A^y/A – the relative rate of amplitude changes.

Thus, the shift of the Poynting zero of the transversal component is determined by the following factors: the phase changes gradient of the referent beam, the gradient

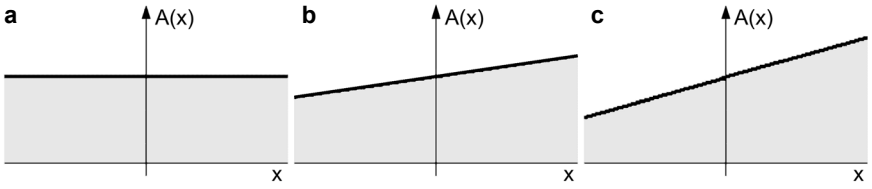

Fig. 14. The example of field parameters changes (amplitude changes); **a** – the beam without asymmetry, **b** – the "insignificant" asymmetry, **c** – the "significant" asymmetry.

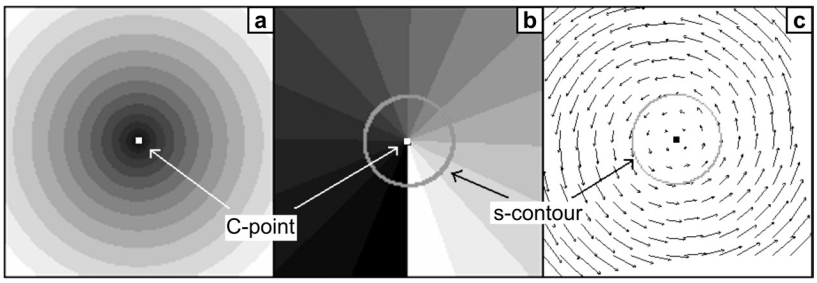

Fig. 15. The behavior of the transversal component of the Poynting vector in the area of *C*-point for superposing beam without any asymmetry (different colors correspond to different, within 2π, azimuths); **a** – corresponds to the distribution of the transversal component modulus of the Poynting vector, **b** – illustrates the behavior of its azimuth; **c** – illustrates the joint behavior of the modulus and azimuth of the Poynting vector (orientation and magnitude of the vector are represented by the direction and length of arrows, respectively).

of relative changes of its amplitude, and by the ratio of the intensities of vortex and reference waves.

The influence of the asymmetry was considered in the area which coincides with the vortex core [7]. Therefore, the linear approximation was satisfied for the amplitude and phase changes of a beam. Figure 14 illustrate such changes of the amplitude. The phase changes of a reference beam have a similar character.

Note that the goal of this paper is to recognize general tendencies of the Pointyng vector behavior in the area of elementary polarization singularities. Therefore, strict estimations will be done in future papers. Here we used rather "indistinct" notions for the description of a reference beam like "insignificant" and "significant" asymmetries of its parameters. As "insignificant" asymmetry of a phase and an amplitude we took the magnitudes of the phase and amplitude gradients, which are less than $\pi/2$ and less than 0.5, respectively.

As it follows from Eq. (12), the location of the singularity depends also on the intensity of a reference beam. More exactly, the location of such point depends on the ratio between the intensities of a vortex and reference beams. However, accordingly to Eq. (5), the intensity of the vortex beam permanently increases if the point of interest is moved away from the center of the vortex. Therefore, we

characterize the ratio of intensities of the superposing beams by the average intensity along *s*-contour where the amplitudes of both waves are equal. The dimension of *s*-contour increases when such parameters increase too.

The results of computer simulation are presented in Figs. 16–19. Both types of the asymmetry (phase and intensity) were introduced in *x*-direction alone. The results of computer simulation for the beams without asymmetry are presented in Fig. 15 for comparison.

The singularity point coincides with the position of *C*-point. The *s*-contour is the regular circle. Figure 15**a** corresponds to the distribution of the transversal component modulus of the Poynting vector. Figure 15**b** illustrates the behavior of its azimuth. Different colors correspond to different (within 2π) azimuths. Figure 15**c** presents the joint behavior of the modulus and azimuth of the Poynting vector. Orientation and magnitude of the vector are represented by the direction of arrows and their length, respectively.

Figure 16 illustrates the shifts of the Poynting singularity under the influence of the phase asymmetry. The shift magnitude increases if the phase gradient of the reference beam also enlarges. The shape and the dimension of *s*-contour and the location of *C*-point remain without any changes in respect to the previous case.

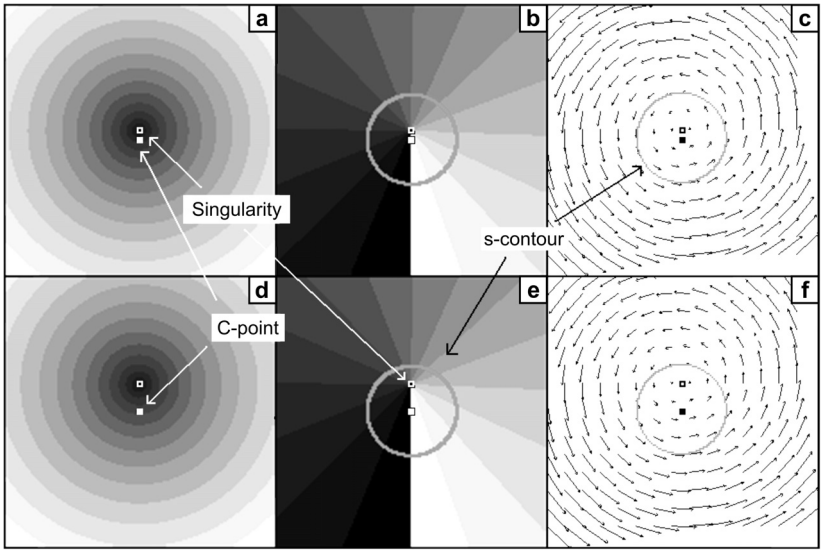

Fig. 16. Shifts of the Poynting singularity under the influence of the phase asymmetry of the reference beam; **a**, **b**, **c** – the "insignificant" phase asymmetry of the referent beam (modulus of the phase gradient is equal to $\pi/4$); **d**, **e**, **f** – the "significant" phase asymmetry of the reference beam (modulus of the phase gradient is equal to $3\pi/4$; **a**, **d** correspond to the distribution of the transversal component modulus of the Poynting vector; **b**, **e** illustrate the behavior of its azimuth (different colors correspond to different, within to 2π, azimuths); **c**, **f** illustrate the joint behavior of the modulus and azimuth of the Poynting vector (orientation and magnitude of the vector are represented by the direction and length of arrows, respectively).

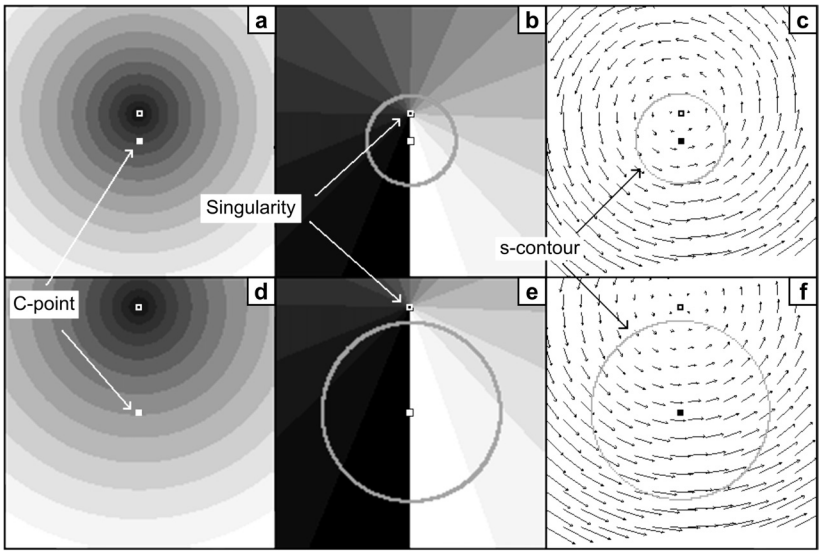

Fig. 17. The influence of the phase asymmetry for the same magnitudes of the phase gradient (modulus of phase gradient is equal to $3\pi/4$) and different ratios between vortex and reference beams. Intensity of the reference beam in the case **d**–**f** exceeds intensity of the regular beam (case **a**–**c**) by 4 times. Case **a** and **d** correspond to the distribution of the transversal component modulus of the Poynting vector. Case **b** and **e** illustrate the behavior of its azimuth. Different color correspond to different (within 2π) azimuths. Case **c** and **f** illustrate the joint behavior of the modulus and azimuth of the Poynting vector. Orientation and magnitude of the vector are represented by the direction and length of arrows, respectively.

As it is seen from the figures, the shift of the singularity position is observed in "*y*-direction" (accordingly to Eq. (12)), due to the fact that phase asymmetry was introduced in "*x*-direction".

Figure 17 presents the influence of the phase asymmetry for the same magnitudes of the phase gradient (its magnitude is equal to $3\pi/4$) and different ratios between the vortex and reference beams. Figures 17**d**–17**f** correspond to the intensity of the reference beam, which exceeds 4 times the intensity of the regular wave used in the case **a**–**c**. The dimension of *s*-contour increased twice. At the same time, the singularity shift in the case **d**–**f** exceeds the shift associated with the case **a**–**c** 4 times. It is interesting that for the second intensity level of the reference beam the position of the Poynting singularity is shifted to the area with another rotation direction of a field vector (handedness factor h changes its sign under the crossing of the *s*-contour).

The influence of the intensity asymmetry on the position of the Poynting singularity is illustrated in Fig. 18. It is seen that the intensity asymmetry of the reference beam results in the transformation of the *s*-contour shape, depending on the intensity modulation of the regular wave. The shift of singularity is observed in the direction (*x*-direction), which corresponds to the direction of the intensity modulation of the reference beam. Figures 18**d**–18**f** correspond to the intensity gradient of the

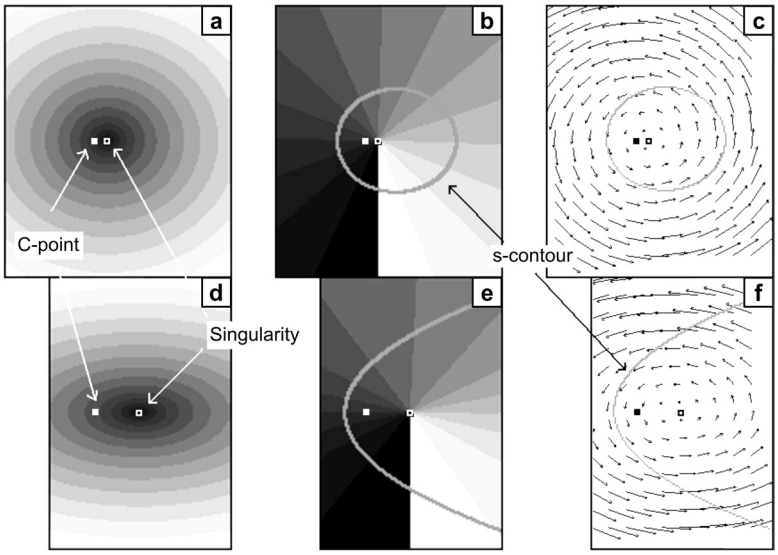

Fig. 18. Shifts of the Poynting singularity under the influence of the amplitude asymmetry of the reference beam; **a**, **b**, **c** – the "insignificant" amplitude asymmetry of the referent beam (modulus of the amplitude gradient is equal to 0.5); **d**, **e**, **f** – the "significant" amplitude asymmetry of the referent beam (modulus of the amplitude gradient is equal to 1). Cases **a** and **d** correspond to the distribution of the transversal component modulus of the Poynting vector. Cases **b** and **e** illustrate the behavior of its azimuth. Different colors correspond to different (within 2π) azimuths. Cases **c** and **f** illustrate the joint behavior of the modulus and azimuth of the Poynting vector. Orientation and magnitude of the vector are represented by the direction and length of arrows, respectively.

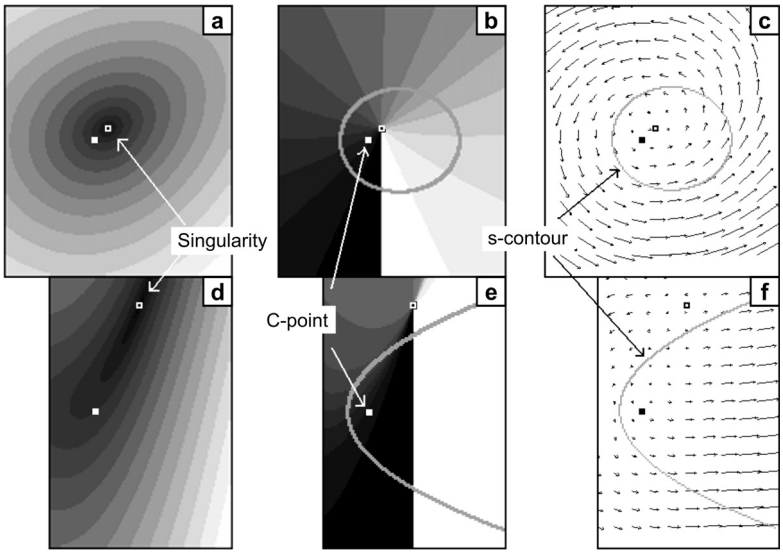

Fig. 19. Shifts of the Poynting singularity under the influence of both kinds of asymmetry (phase and amplitude) simultaneously.

reference beam, which exceeds 4 times the intensity of the regular beam used in the case **a**–**c**. At the same time, the singularity shift in the case **d**–**f** increases only twice in respect to the shift associated with the case **a**–**c**.

Figure 19 presents the shifts of the Poynting singularity under the influence of both kinds of asymmetry (phase and amplitude) simultaneously. Due to such changes of the reference beam, the shift of the singularity point takes place in both *x*- and *y*-directions. It has been noted that the magnitude of this "joint" shift is more than "summary" shift associated with the vector sum of the corresponding shifts resulting from "pure" phase and amplitude asymmetries. It is seen from Figs. 19**d**–19**f** that the singularity point shifts even to the area with another rotation direction of a field vector.

7. Conclusions

The following conclusions can be derived from conducted studies:

1. Averaged angular momentum appears in the *C*-point vicinity when the signs of the topological charge of the vibration phase and handedness factor are different and it is equal to zero when the signs are the same. The position of vortex singularity associated with the transversal component of the averaged Poynting vector coincides with the position of *C*-point.

2. Generally the positions of the singularities of the transversal Poynting vector component do not coincide with the *C*-points location. The shift of the Poynting singularities relatively to *C*-points is defined by the ratio between phase gradients and the ratio of amplitude gradients associated with the orthogonally polarized components of a field.

References

[1] LANG M.J., BLOCK S.M., *Resource Letter: LBOT-1: Laser-based optical tweezers*, American Journal of Physics **71**(3), 2003, pp. 201–15.

[2] ALLEN L., PADGETT M.J., BABIKER M., *The orbital angular momentum of light*, [In] *Progress in Optics*, [Ed.] Wolf E., Vol. 39, Elsevier Science B.V., New York 1999, pp. 291–372.

[3] MOKHUN I., BRANDEL R., VIKTOROVSKAYA JU., *Angular momentum of electromagnetic field in areas of polarization singularities*, Ukrainian Journal of Physical Optics **7**(2), 2006, pp. 63–73.

[4] BERRY M., *Paraxial beams of spinning light*, Proceedings of SPIE **3487**, 1998, pp. 6–11.

[5] ALLEN L., PADGETT M.J., *The Poynting vector in Laguerre–Gaussian beams and the interpretation of their angular momentum density*, Optics Communications **184**(1–4), 2000, pp. 67–71.

[6] BERRY M.V., *Phase vortex spirals*, Journal of Physics A: Mathematical and Theoretical **38**(45), 2005, pp. L745–51.

[7] NYE J.F., *Natural Focusing and Fine Structure of Light: Caustics and Wave Dislocations*, Institute of Physics Publishing, Bristol, Philadelphia 1999.

[8] ANGELSKY O., BESAHA R., MOKHUN A., MOKHUN I., SOPIN M., SOSKIN M., VASNETSOV M., *Singularities in vectoral fields*, Proceedings of SPIE **3904**, 1999, pp. 40–54.

[9] MOKHUN I., ARKHELYUK A., BRANDEL R., VIKTOROVSKAYA JU., *Angular momentum of electromagnetic field in areas of optical singularities*, Proceedings of SPIE **5477**, 2004, pp. 47–54.

[10] ANGELSKY O., MOKHUN A., MOKHUN I., SOSKIN M., *The relationship between topological characteristics of component vortices and polarization singularities*, Optics Communications **207**(1–6), 2002, pp. 57–65.

[11] FREUND I., SHVARTSMAN N., FREILIKHER V., *Optical dislocation networks in highly random media*, Optics Communications **101**(3–4), 1993, pp. 247–64.

[12] NYE J.F., *Polarization effects in the diffraction of electromagnetic waves – the role of disclinations*, Proceedings of the Royal Society A: Mathematical and Physical Sciences **387**(1792), 1983, pp. 105–32.

[13] HAJNAL J.V., *Singularities in the transverse fields of electromagnetic waves. I – Theory. II – Observations on the electric field*, Proceedings of the Royal Society A: Mathematical and Physical Sciences **414**(1847), 1987, pp. 433–68.

Received February 2, 2007